MEASUREMENT OF DOUBLE DIFFERENTIAL CROSS-SECTIONS FOR LIGHT CHARGED PARTICLES PRODUCTION IN NEUTRON INDUCED REACTIONS AT 62.7 MeV ON LEAD TARGET

M. Kerveno, F. Haddad, P. Eudes, T. Kirchner, C. Lebrun
SUBATECH, Nantes, France

I. Slypen, J.P. Meulders
Institut de Physique Nucléaire, Louvain-la-Neuve, Belgique

V. Corcalciuc
Institute of Atomic Physics, Bucharest, Roumania

C. Le Brun, F.R. Lecolley, J.F. Lecolley, M. Louvel, F. Lefèbvres
Laboratoire de Physique Corpusculaire de Caen, Caen, France

Abstract

In the framework of nuclear waste transmutation, we have measured $d^2\sigma / d\Omega dE$ for protons, deuterons, tritons and alpha production in neutron induced reactions on a lead target. Due to the structure of the neutron beam, incident neutron energies between 30 and 62.7 MeV have been obtained at once. The analysis of 62.7 MeV neutron is now complete for hydrogen isotopes and a first set of comparisons has been done with calculations. On one hand, it is found that the GNASH-ICRU data do not give the correct cross-sections (neither absolute value nor shape). In the other hand, a comparison for protons using FLUKA is working reasonably well except an underestimation of the pre-equilibrium emission around 30 MeV at forward angles and an overestimation of thermal emission at backward angles. Further data on protons induced reactions at the same energy, obtained within an European concerted action, will be available soon allowing a stronger constraint on theoretical calculations.

1. Introduction

The renewal interests on intense neutron source have put forward the necessity of new sets of nuclear data. This is particularly true, in the intermediate energy range between 20 and 200 MeV, for the development of new options for nuclear waste management based on the concept of hybrid system which combines an intense high energy proton beam with a sub-critical fission reactor. One important point of these studies is to know precisely the characteristics of the nuclear reactions taking place in the spallation target that is intended to be in Pb-Bi or Hg. In particular, it's necessary to estimate, in reactions induced by neutrons, the production of light charged particles (lcp) which may have critical effects on materials.

At present, code calculations are used to simulate these phenomena. Below 20 MeV, the upper limit of the databases, codes provide results with a good level of confidence. Above 150 MeV, Intra Nuclear Cascade calculations provide also good results. On the contrary, in the intermediate energy region where the pre-equilibrium emission is important, new theoretical approaches seem to be necessary to ensure a good link between low and high-energy processes.

These new approaches based on pre-equilibrium models will allow increasing the upper limit energy value (from 20 to 150 MeV) of data bases providing that theoretical codes could have sufficient predictive power in this energy range. Thus it's necessary to measure new cross-sections to constrain these codes in order to improve their predictive power and to evaluate the quantity of hydrogen and helium isotopes that will be emitted from the lead target and eventually estimate their interactions with structure materials. A large concerted program of nuclear data measurements is now carrying out by several French and European laboratories to measure double differential cross-sections production for light charged particles in neutron induced reactions on different targets.

We report hereby double differential cross-sections for protons, deuterons and tritons production from a lead target at 62.7 MeV incident neutron energy.

2. Experimental set-up

The experiment has been done at the fast neutron facility existing at the cyclotron CYCLONE at Louvain-la-Neuve [1]. The neutron beam is obtained using the $^{7}Li(p,n)^{7}Be_{gs}$ (Q = -1.644 MeV) and $^{7}Li(p,n)^{7}Be^{*}$ (Q = 0.431MeV) reactions. The neutron facility is presented in Figure 1. The important features of this line are the presence of a beam peak off, BPO, upstream the lithium target to get the time at which the neutrons are created and a faraday cup which collect the non-interacting deflected protons. The scattering chamber is located 3.28 m after the neutron production point and is followed by a second chamber which contains a second beam monitor system.

Figure 1. **Global view of the experimental set-up**

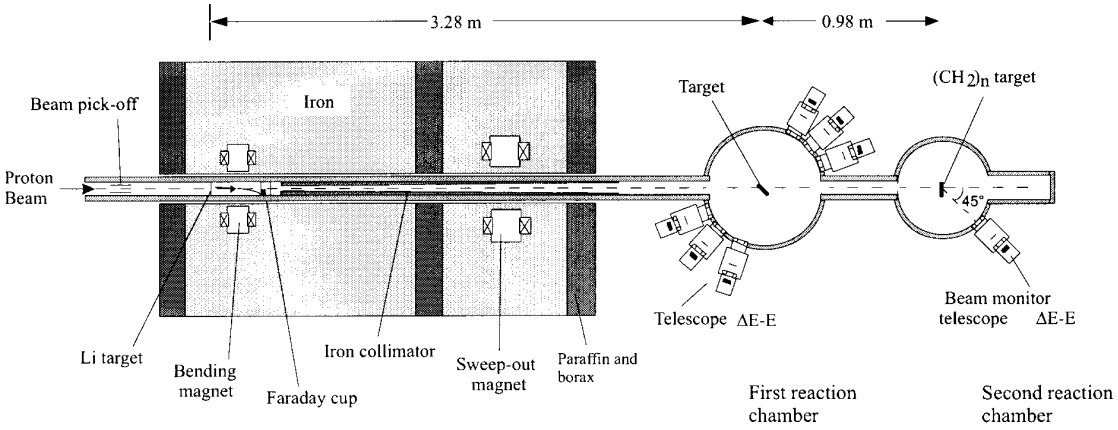

About 10^6 n/s are available in the reaction chamber when a 10μ A proton beam interacts on a 3 mm thick natural lithium target [2]. The neutron spectrum is presented in Figure 2. It consists of a well-defined peak located at 62.7 MeV containing about 50% of the neutrons and a flat continuum at low neutron energy, which is 8 times lower than the peak maximum. The full width at half maximum of the peak is 4 MeV. The neutron beam spot is quite large at the reaction point as shown in the inset of Figure 2 that presents the radial neutron distribution normalised to the intensity on the centre.

Figure 2. **Neutron spectrum produced by a 65 MeV protons beam on a lithium target. The inset shows the beam profile, normalised to the centre intensity, 3 m downstream the lithium target.**

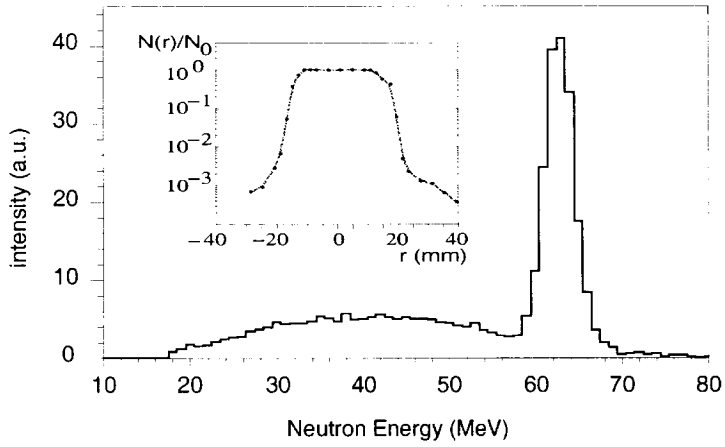

The experimental set-up is based on the one used by the group of J.P. Meulders [3,4]. The reaction chamber allows to use simultaneously six telescopes. Each telescope is composed of a ΔE detector (100 μm thick and 4 cm in diameter NE102 plastic scintillator) and an E detector (22 mm thick and 38.1 mm in diameter CsI crystal). A set of two collimators is inserted in the telescope as shown in Figure 3 to precisely define the detection solid angle. The ΔE detector gives a fast time signal, which allows time of flight measurement and ensures a good reconstruction of the incident neutron energy. The CsI thickness has been optimised to stop the light charged particles produced in our experiment and a pulse shape analysis of the signal is performed.

Figure 3. **Schematic view of a telescope**

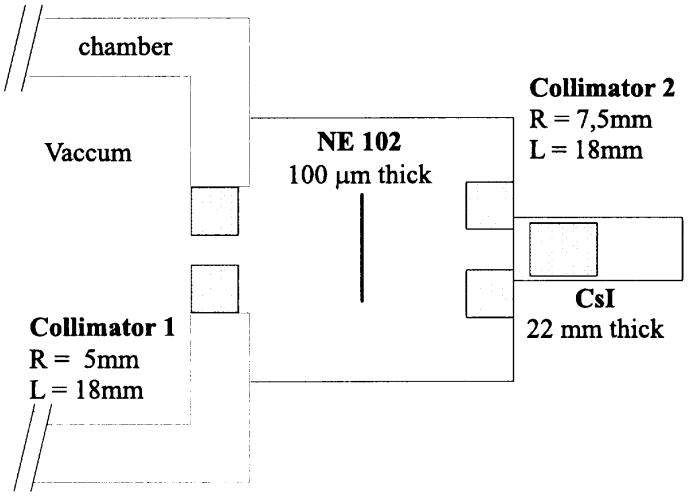

During the experiment, a quite complete angular distribution has been obtained from 20° to 70° by step of 10° in the forward hemisphere and at 110° and 160° in the backward hemisphere. Two different configurations have been used to allow two times longer recording data time at backward angles.

3. Data analysis

The particle identification is obtained by performing a pulse shape discrimination of the CsI detector signal. Plotting the slow (CsI_s) versus the fast (CsI_f) component of the CsI light output allows to separate the different hydrogen isotopes as well as the helium. As shown on Figure 4, the good quality of the discrimination added to the possibility to suppress most of the background (neutron and γ) using the ΔE-E correlation facilitates the particle identification.

Figure 4. **CsI slow versus fast component of the light output**

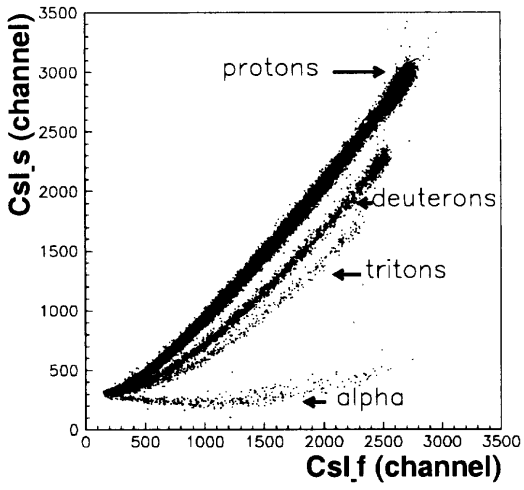

To get the proton (deuteron) energy calibration of our detectors we have used recoil protons (respectively deuterons) from elastic neutron scattering on CH_2 (DH_2) target at 6 different angles from 20^o to 70^o. The time calibration is also extracted from these data.

Figure 5. **Total time of flight as a function of the measured energy for alpha particles in a lead run**

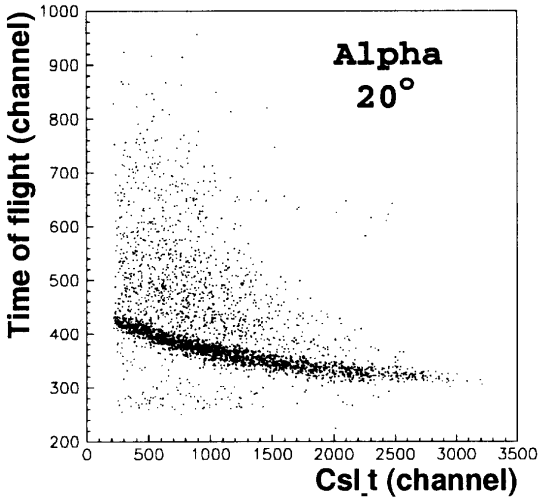

The triton and the alpha calibration have been performed using the time of flight information available for these particles, following the relation $T_{cp} = T_{tot} - T_n$ where T_{tot}, corresponds to the measured time between the BPO and the ΔE signals, T_n to the time made by the neutron to go from the BPO to the target and T_{cp} to the time of flight of the particle from the target to the ΔE detector. The special neutron beam energy distribution (see Figure 2) allows selecting only the neutrons from the peak. The bi-parametric plot shown on Figure 5 presents T_{tot} versus the measured energy in channel for alpha particles in a lead run. A clear band appears corresponding to the 62.7 MeV incident neutrons for which T_n is known. For several points on this band, it is then possible to extract the alpha particle energy from T_{cp} and to determine the energy calibration curve. The same method applies also for the other kind of particles. In particular, the calibration obtained by this method for protons and deuterons gives similar results as the first method based on elastic scattering. In Figure 6, calibration curves used for telescope 1 are summarised for isotopes under study.

Figure 6. **Calibration curves used for telescope 1. Proton corresponds to the full black line, deuteron to the dashed line, triton to the dotted line and alpha to the dashed-dotted line.**

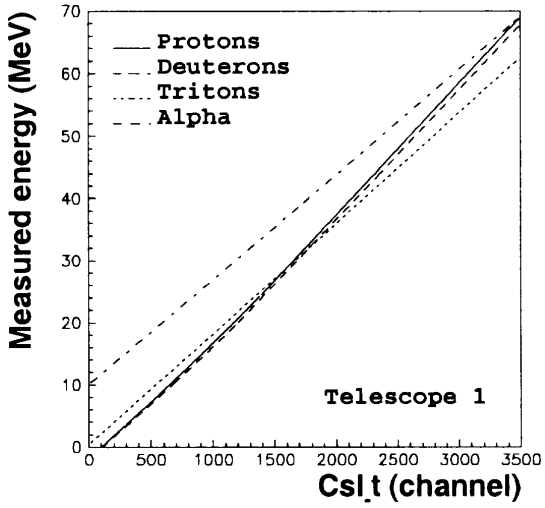

Using the calibration curves, it is possible, event by event, to determine the lcp energy and then T_{cp} to deduce T_n and the neutron energy. As an illustration, in Figure 7, the total deuteron spectrum is plotted as a function of energy. The inset of Figure 7 shows the reconstituted neutron incident energy distribution. By selecting a slice in the neutron spectrum, the deuteron spectrum can be obtained for the corresponding neutron incident energies. As examples, deuterons created by neutrons of 62.7 MeV (respectively 43 MeV) are represented as hashed histogram (squared histogram). It is then possible in one experiment using 65 MeV protons to measure cross-sections at neutron incident energy ranging from 30 MeV to 62.7 MeV.

Figure 7. **Deuteron spectrum obtained by selecting 62.7 MeV (respectively 43 MeV) incident neutron energy is presented as hashed (squared) histogram**

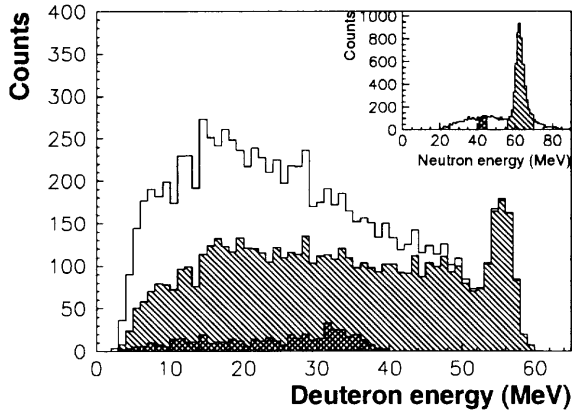

The absolute normalisation of the lead double differential cross-section is obtained by using the n-p scattering cross-section extracted from the CH_2 calibration runs [3].

3.1 Corrections

Several corrections have to be made on our data. One concerns the particle scattering on the telescope collimators, the others are coming from the target thickness (0.3 mm). In order to quantify these corrections, we used the GEANT code [5] to simulate as closely as possible the experimental setup and the beam structure.

3.1.1 Diffusion on the collimator set

In Figure 8, the effect of the collimators on a well define energy beam, as shown on the inset of Figure 8, have been plotted. The diffusion leads to a long tail at low energy. The broadening of the peak is due to the energy losses in the target. Using the simulation, it is possible to estimate the pollution of the tail, normalised to the peak population, in each energy bin. Doing these calculations from 5 to 70 MeV allows us to have an estimation of the full diffusion contribution. The iterative correction procedure consists on removing the tail contribution from the spectrum starting from the highest bin: the population of the highest energy bin does not contain any pollution and the corresponding tail contribution can be estimated from the simulation and discarded for each bin of the spectrum.

Figure 8. **Simulation showing the effect of the proton scattering on the collimator set. The inset shows the particle energy before entering our telescope.**

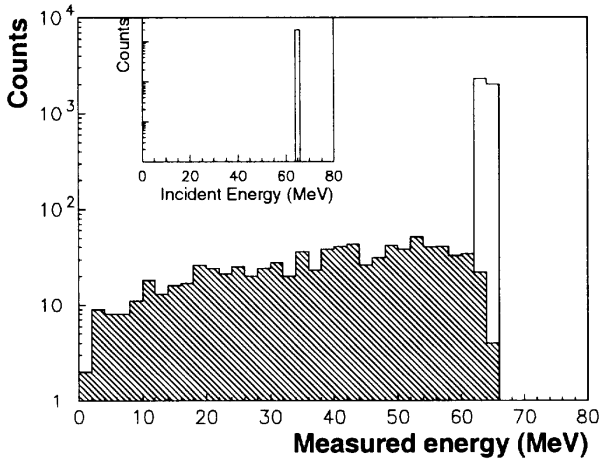

The result of such a procedure is shown on Figure 9 for protons at 20° in the laboratory. The highest spectrum corresponds to the non-corrected one and the lowest one to the corrected one. The effect of the correction is increasing with decreasing energy bin due to the accumulation of corrections coming from higher bins. Such correction corresponds to an overall effect of 13% for protons, 10% for deuterons, 5% for tritons and is negligible for alpha.

Figure 9. **Proton spectrum before and after scattering corrections at 20°.**

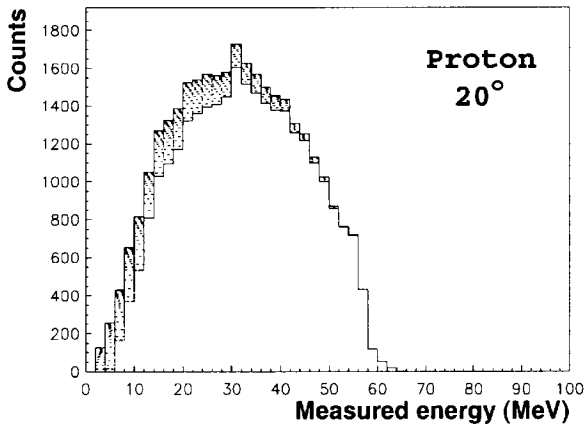

3.1.2 Thick target corrections

Another correction consists of taking into account the energy lost in the target in order to get the emitted energy from the measured energy. In Figure 10, the correlation between emitted energy and mean measured energy is presented for triton and alpha. In both pictures, the dashed line characterises the equality between both energies whereas dots show the effect of our thick lead target. For triton, and the other hydrogen isotopes, the difference is small and of the order of our energy binning. It implies that the correction is a simple shift in energy. On the contrary, the effect for alpha is important and a special method is being developed.

Figure 10. **Emitted energy versus measured energy for triton (left) and alpha (right) for the used target. The dashed line corresponds to no thickness effect.**

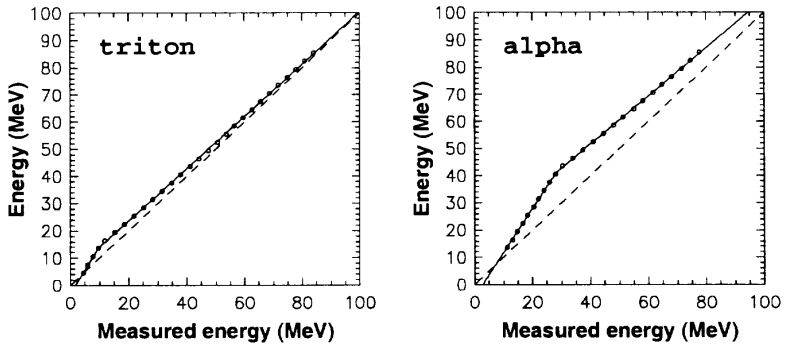

The last correction affects only the low energy particles, which are created without enough energy to cross the entire target and to be detected. This indicates that only the particles created in a fraction of the target, the part close to the output side, can be detected. It is then possible to determine a so-called active target fraction (ATF) which can varied between 0 (nothing can escape) and 1 (everything can escape). The correction depends on the emitted energy and on the type of the particle. Figure 11 shows the evolution of ATF as a function of the emitted energy for tritons and alpha. For hydrogen isotopes, the correction starts below the maximum of the coulomb barrier down to 0 and its effect is small due to the low population. For alpha, this effect goes up to 43 MeV implying a special treatment, which is still under study.

Figure 11. **Active target fraction (see text) as a function of emitted energy.**

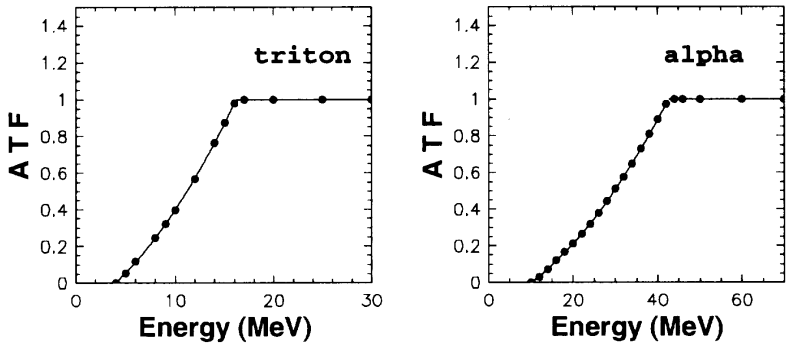

4. Results

Dealing with all these corrections, cross-sections can be extracted for proton, deuteron and triton. Using the Kalbach [6] systematic, it is possible to determine the differential cross-section in energy. Figure 12 presents the dσ/dE for the proton (dots), deuteron (triangles) and triton (square). Energy bins of 2 MeV have been used for proton and deuteron and of 3 MeV for triton. The proton spectrum shows a smooth behaviour with a maximum around 18 MeV. For the deuteron spectrum, the maximum is less pronounced and a small rise appears above 57 MeV due to direct processes. Since our most forward angle is 20°, we do not have enough information to fit properly this part of the spectrum and we decide not to determine the cross-sections above 57 MeV for deuterons. For tritons, the low statistic does not allow us to determine the cross-section above 47 MeV. The integration of these spectra gives a production cross-sections of 290 ± 22 mb for protons, 70 ± 5 mb for deuterons and 24 ± 2 mb for tritons.

Figure 12. **dσ/dE for proton (dots), deuteron (triangles) and triton (squares) in n + Pb at 62.7 MeV.**

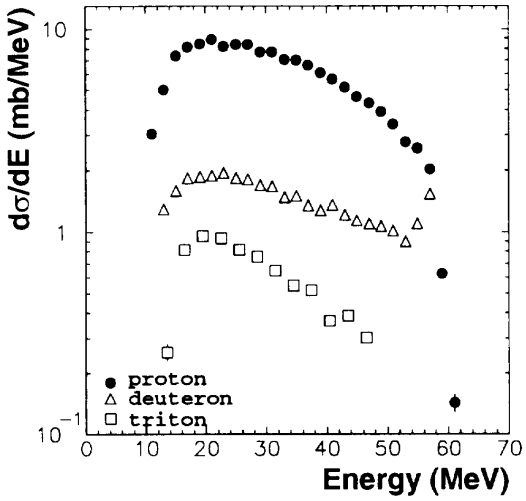

Before starting any comparison with theoretical calculations, it is interesting to compare our experimental results with those found in the literature. No data exists on neutron induced reactions at

this energy and the deuteron data of [7] obtained in proton induced reactions are the only data available to compare with. Since we are looking to deuteron production and that Bi and Pb are neighbours, the production cross-sections in proton and neutron have to be similar in the pre-equilibrium region. On Figure 13, double differential cross-sections are plotted for 20°, 60° and 160°. The black dots correspond to our data and the triangles to the Bertrand and Peelle one [7]. A good agreement is found on the overall angular distribution.

Figure 13. **Deuteron $\frac{d^2\sigma}{dEd\Omega}$ at 20°, 60° and 160°. The dots correspond to neutron induced reaction (this work) and triangles to proton induced reactions [7].**

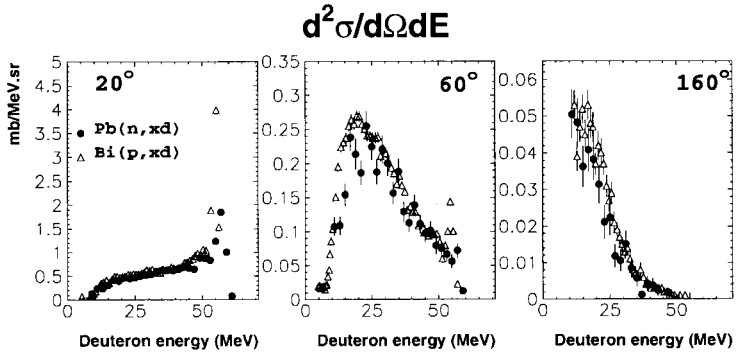

5. Comparison with theoretical calculations

As a first set of comparisons, we used two well-known code FLUKA and GNASH. The GNASH data are coming from a publication of ICRU [8] whereas FLUKA [9] results have been obtained locally. In Figure 14, the double differential cross-sections for protons are reported at 3 different angles. The left column shows ICRU data as dashed line whereas FLUKA data are plotted on the right column as dotted line. In all pictures, the black dots correspond to our data. The ICRU data overestimates, in all spectra, our experimental results. In addition, it presents, at forward angles, a double humped structure localised at low and high energy which is not present in our data that are maximum at medium energy. FLUKA is giving a good total cross-section (270 mb) thanks to the compensation of the underestimation of the medium energy part of the spectrum at forward angles and the overestimation of the low energy part at backward angles. Nevertheless, the shapes of the spectra are in close agreement with the data.

Figure 14. **Proton $\frac{d^2\sigma}{dEd\Omega}$ for n + Pb at 62.7 MeV. Dots are the experimental data whereas curves in the left (right) column correspond to ICRU [8] (FLUKA [9]) results.**

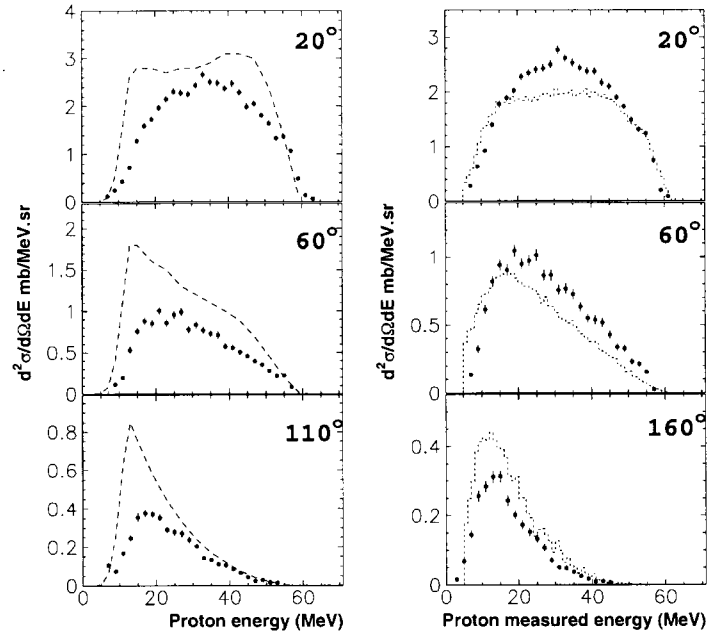

For composite particles such as deuterons, the discrepancy is greater as is shown on Figure 15 where the dashed line corresponds to ICRU data and black dots to our experimental data.

Figure 15. **Deuteron $\frac{d^2\sigma}{dEd\Omega}$ for n + Pb at 62.7 MeV. Dots are the experimental data whereas curves correspond to ICRU [8] results.**

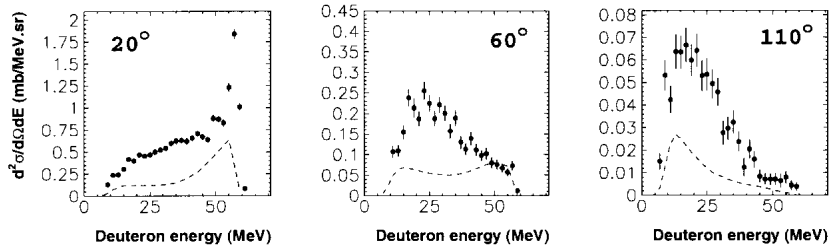

6. Conclusion

Proton, deuteron and triton double differential cross-sections have been measured in 62.7 MeV neutron-induced reactions on natural lead target. A special attention has been devoted to the correction procedures coming from our use of thick target and collimators. Measurements were done with a good statistic and are in good agreement with data of [7]. The comparison with some well-known theoretical data from GNASH-ICRU and FLUKA shows some disagreements. The largest differences are found for GNASH-ICRU that neither reproduces the shape of the spectra nor the

absolute values of proton spectra. The composite particles are also not correctly reproduced. FLUKA is giving a good total cross-section value thanks to differences cancelling each other at forward and backward angles. Further comparisons with theoretical approach are underway especially with model including pre-equilibrium emission such as MINGUS [10]. Other data on lead using proton-induced reactions at the same energy beam are under analysis and will be delivered soon to enrich the data tables.

This work has been supported by the European Commission under the concerted action N°FI4I-CT98-0017 and by the GDR GEDEON (research group CEA – CNRS – EdF – FRAMATOME).

REFERENCES

[1] A. Bol, P. Leleux, P. Lipnik, P. Macq and A. Ninane, *A Novel Design for a Fast Neutron Beam*, NIM, 1983, 214, 169-173.

[2] I. Slypen, V. Corcalciuc and J.P. Meulders, *Geometry and Energy Loss Features of Charged Particle Production in Fast-neutron Induced Reactions*, NIMB, 1994, 88, 275-281.

[3] I. Slypen, V. Corcalciuc and J.P. Meulders, *Proton and Deuteron Production in Neutron-induced Reactions on Carbon at E_n = 42.5, 62.7 and 72.8 MeV*, Phys. Rev. C, 1985, 51, 1303-1311.

[4] S. Benck, I. Slypen, V. Corcalciuc and J.P. Meulders, *Light Charged Particle Emission Induced by Neutrons with Energies Between 25 and 65 Mev on Oxygen I. Protons and Deuterons*, Eur. Phys. J. A., 1998, 3,149-157.

[5] *GEANT: Detector Description and Simulation Tool*, CERN program library long write-up W5013.

[6] C. Kalbach, *Systematic of Continuum Angular Distributions: Extensions to Higher Energies*, Phys. Rev. C, 1988, 37, 2350-2370.

[7] F.E. Bertrand and R.W. Peele, *Complete Hydrogen and Helium Particle Spectra from 30 to 60 Mev Proton Bombardment of Nuclei With A = 12 to 209 and Comparison with the Intranuclear Cascade Model*, Phys. Rev. C, 1973, 8, 1045-1064.

[8] **I**nternational **C**ommission on **R**adiation **U**nits and **M**easurements, *Nuclear Data for Neutron and Proton Radiotherapy and for Radiation Protection*, reports 63, 1999.

[9] A. Ferrari and P.R. Sala, *A New Model for Hadronic Interaction at Intermediate Energies for the FLUKA Code*, The MC93 international conference on Monte Carlo Simulation in High Energy and Nuclear Physics, Tallahassee, Florida, 1993, 277-288, World scientific, Singapore.

[10] A.J. Koning, M.B. Chadwick, *Microscopic Two-component Multistep Direct Theory for Continuum Nuclear Reactions*, Phys. Rev. C, 1997, 56, 970-99.